Scaling Laws for Electromagnetic Launchers Considering an Existing Pulse Power Supply

Scaling Laws for Electromagnetic Launchers Considering an Existing Pulse Power Supply

Görkem Gülletutan, Ozan Keysan
Department of Electrical and Electronics Engineering
Middle East Technical University
Ankara, Turkey
keysan@metu.edu.tr

Nail Tosun
Electrical Power Group
Newcastle University
Newcastle Upon Tyne, NE1 7UR, United Kingdom
n.tosun2@newcastle.ac.uk

Ferhat Yurdakonar, Baran Yıldırım, Zeynep Çöklü, Mustafa Karagöz
Defence System Technologies Business Sector
ASELSAN Inc.
Ankara, Turkey
mkaragoz@aselsan.com.tr

***Abstract*—In all areas of engineering, testing full-scale models can be both costly and risky and often not necessary. The scaling laws can be implemented in electromagnetic launchers (EMLs). The objective is to obtain similar temperatures, magnetic induction, and stress fields (T, B, and S) compared to the full-size geometry. A few EML dimensions, such as its cross-section, rail separation, and length, must be scaled appropriately to obtain accurate results. Pulsed power supply (PPS) parameters require adjustments as well. However, designing a new PPS prototype requires considerable engineering time and budget. Therefore, in this study, scaling rules are studied utilizing an existing PPS. EMFY-4, a recently developed EML with a 50 x 60 mm concave bore and 6-m length, is scaled to be used with a 250 kJ capacitive PPS. A multi-objective optimization study is conducted to get the best design. The first objective is to get a minimum rail length to seek higher energy density. The second objective is to minimize the muzzle current to the peak rail current ratio for higher efficiency. The effect of armature mass, capacitor charging voltage, and the required number of PPS modules on the objective functions are discussed. The study showed that when the existing PPS is used, the scaling with the higher scaling factor, denoted as (λ), gives better results.**

***Index Terms*—Railgun, electromagnetic modeling, scaling laws.**

I. Introduction

Electromagnetic launchers (EMLs) convert electrical energy to linear kinetic energy. It has an armature, projectile, and two conducting rails. A pulsed-power supply (PPS) generates a few MA pulse-shaped current in milliseconds. Lorentz force affects the armature, the propulsion mechanism.

Testing full-scale EMLs is expensive, dangerous, and time-consuming. Scaled versions of EMLs can be used to test several engineering and design problems. Scaling EMLs makes following experimental studies considerably quicker and less expensive;

1) *Electrical contact examinations*: Obtaining stable electrical contact is a challenging issue. Muzzle voltages can be utilized to examine contact conditions [1]. However, repeated launch tests are required more often i.e., to examine the rail life. A scaled-down EML can lead to more rapid experiments, as simply replacing rails after launches becomes more practical, tests can be done indoors, etc.
2) *Material studies*: Cutting-edge materials are required for numerous reasons to ensure a safe launch [2]. For example, most EMLs suffer from the degradation of their insulators [3], so any improvement in the insulation material will directly increase the rail life. However, experimenting with multiple material options is time-consuming because mechanical support structure must be removed each time insulators are changed. Unfortunately, insulation is not the only part of the EML which suffer from reliability. Resistive claddings with different materials offer the potential for increased rail life [4].

All of these studies rely heavily on experimental results, which can be challenging to test on a full-scale prototype.

Studies on the scalability of EMLs have been published for many years. The goal of the scaling study should be to maintain constant temperature, magnetic, and stress fields (T, B, and S) relative to the full-scale model. However, this condition brings some requirements, as Yun states [5]. Those requirements are remarked by several scaling factors such as; λ_t, λ_x, λ_I, λ_m denoted as time, geometry, current, and mass scaling factors as in (1), where $(.)$ indicates the scaled model parameters, t_{exit} represents the armature exit time, h is the rail height, and I_r is the rail current, and m is the armature mass respectively.

$$\lambda_t = \frac{\bar{t}_{exit}}{t_{exit}}, \quad \lambda_x = \frac{\bar{h}}{h}, \quad \lambda_I = \frac{\bar{I}_r}{I_r}, \quad \lambda_m = \frac{\bar{m}}{m} \tag{1}$$

To give an example of Yun's restrictions [5], λ_t should be equal to the square of the λ_x and, λ_I should be linearly proportional with λ_x as in (2). In order to demonstrate the

efficacy of these scaling rules, the rail pressures of scaled and non-scaled models can be compared.

$$\lambda_t = \lambda_x^2$$
$$\lambda_I = \lambda_x \tag{2}$$

EMLs use a system of two rails with opposing currents, which results in a seperating force between them. A 50×60 mm caliber with $I_r = 2$ MA, creates 252 MPa rail pressure. With $\lambda = \lambda_I = \lambda_x = 0.4$, the resulted 20×24 mm caliber with $I_r = 800$ kA produces identical rail pressure. This is shown in Fig. 1.

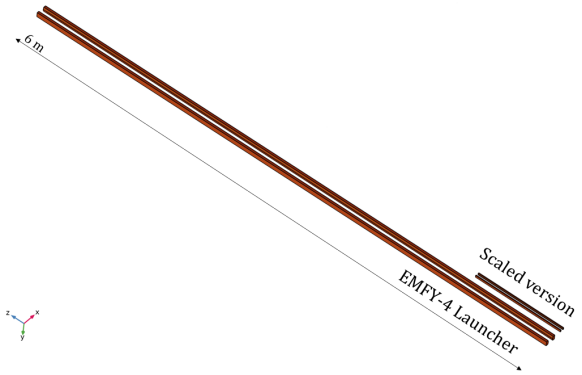

Fig. 1. The view of the reference and scaled model with λ is equal to 0.4. The rail length of the scaled model is not associated with λ and is scaled for illustration purposes.

Additional requirements can be added to obtain more similarities. For example, (3) can be enforced to make muzzle velocities, denoted as v_{exit}, equal. In this particular case, the rail length, denoted as l_r, is not scaled by any rule. Only one unique l_r satisfies the (T,B,v, S) similarity.

$$\lambda_m = \lambda_x^4 \tag{3}$$

Although early works [5], [6] provide a solid understanding of scaling problems in EML, they did not consider PPS parameters. Energy is supplied to the system with an ideal-controllable current source. However, in practice, multiple PPS units have consecutively energized the bore. Zhang *et. al.* [7] extended these scaling rules to the capacitive PPS parameters. There are multiple nonlinearities reported and corrected by peers; stress field dis-match [8], variations due to diffusion process [9], hypervelocity drag forces [10], and most of them are reviewed by Sung *et. al.* [11]. By modifying the capacitance and inductance values of the PPS, these studies scale the rail-current waveform in both the amplitude and time domains. This can be seen in Fig. 2 with reference and perfectly scaled reference models. This procedure necessitates an expensive new PPS unit design.

In this article, we performed a scaling study, which is unavailable in the literature. Rather than designing and manufacturing a new PPS unit for a scaling study, already-existing PPS unit is utilized for EML scaling study.

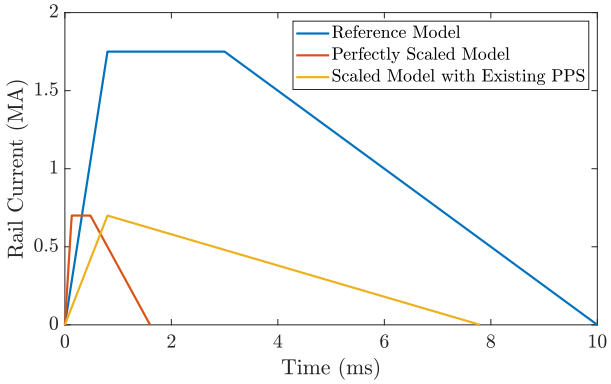

Fig. 2. The current waveform of the reference model, perfectly scaled model, and the scaled model with the existing PPS.

II. Reference Prototypes

ASELSAN's last EML prototype, EMFY-4, has a 50×60 mm concave caliber and 6 m length. In the study, it is taken as the reference design. The parameters of the recently developed EMFY-4 launcher are shown in Table I. The parameters of the 250 kJ capacitive PPS unit is presented in Table II.

TABLE I
Geometric Parameters of the Launcher[1].

Rail Height (mm)	50
Rail Separation (mm)	60
Rail Length (m)	6

[1] The precise geometry of the convex shape of the rails is not disclosed due to their confidential nature.

TABLE II
Parameters of a 250 kJ Capacitive-PPS.

	Description	**Value**
C	Capacitance of the capacitor bank	4 mF
R_C	ESR of the capacitor bank	0.25 mΩ
L_C	ESL of the capacitor bank	0.1 μH
L_{PPS}	Inductance of the pulse shaping inductor	20 μH

III. Simulation Model

To reduce computing cost in complex simulations, we propose a 1-D numerical tool over a 3-D one. Simplifying the problem to a single dimension reduces computing power and memory utilisation, speeding up the analysis without affecting accuracy. Meta-heuristic optimisation studies benefit from this since fitness evaluations are time-consuming. The simulation model is demonstrated in Fig. 3 where the barrel is modelled with dynamic inductance and resistance.

IV. Scaling Methodology

L', is one of the most important parameters to determine EML efficiency. Kerrisk's formula is a popular method for calculating L', which requires three inputs: s, w, and h [13]. The formula applies exclusively to rectangular rails, but also it yields close results for convex rails. This is shown in Table III.

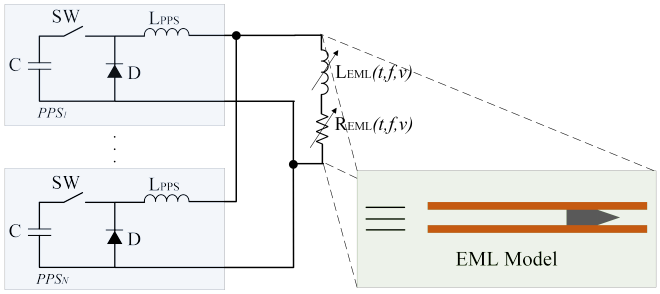

Fig. 3. 1-D simulation model. The detailed discussion can be found in [12]

TABLE III
L' VALUES OF THE REFERENCE MODEL AND THE SCALED MODEL WITH $\lambda = 0.4$ FOR BOTH CONVEX AND RECTANGULAR RAILS.

	Convex Rails	**Rectangular Rails**
Reference Model	0.567 uH/m	0.530 uH/m
Scaled Model	0.559 uH/m	0.527 uH/m
Difference	1.42%	0.57%

When the desired v_{exit} in the scaled model is the same as the reference model, armature mass can be used to control the scaled rail length [11]. Therefore, rail length is excluded from the geometric entities to be scaled with λ.

As stated in [12], VSE resistance is proportional to h, hence with λ_x. The Lorentz force on the armature is found as in (4). With scaling, L' does not change, and the I_r changes with λ to keep linear current density constant which is defined in (5). Therefore, F changes with λ^2.

$$F = \frac{L' I_r^2}{2} \tag{4}$$

$$J = \frac{I_r}{h} \tag{5}$$

As stated in [11], if the EML is completely scaled, the t_{exit} and m relationships between the scaled model and reference model as in (2) and (3) are valid to have the same v_{exit} in both models. Nonetheless, this argument depends on the fact that I_r is scaled in both magnitude and time.

In this article, the PPS is not scaled; thus, the t_{rise} can not changed with λ. This is shown in Fig. 2. Therefore, (3) is invalid.

The mass relationship is determined by considering the specific action integral, g, shown in (6) where $\mathrm{A_c}$ specifies the minimum cross-sectional area that the armature should have. This parameter is essential for launch safety and is frequently used to determine armature size. The specific armature action value (g) is calculated as 19500 ± 2400 $\mathrm{A^2 s/mm^4}$ for Al-7075 in [14].

$$g = \frac{\int I_r^2 dt}{A_c^2} \tag{6}$$

The required minimum armature mass $\bar{m}$ is a constraint to keep g constant in scaled models with the reference model. The action value is kept in the range when (7) is provided.

$$\bar{m} = m\lambda^3 \tag{7}$$

V. OPTIMIZATION STRATEGY

This study used NSGA-II for multi-objective optimisation. It addresses several competing goals using rapid non-dominated sorting and crowding distance calculation [15]. The flowchart of NSGA-II algorithm is demonstrated in Fig 4.

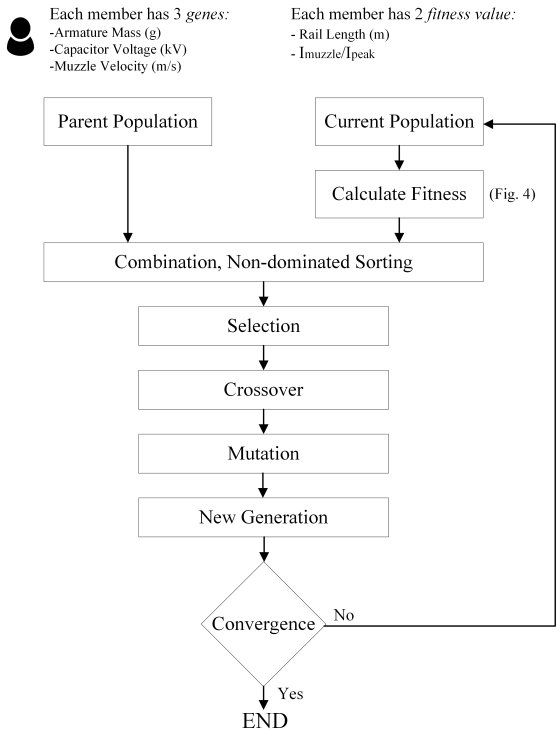

Fig. 4. The flowchart of NSGA-II algorithm.

The optimization study can be formulated as in (8). Objectives are to minimize the rail length (l_r) and the ratio of the exit current (I_{exit}) to the peak current (I_{peak}), which seeks the minimum volume/mass prototype, maximum energy density, and maximum efficiency.

$$\begin{aligned} \text{min} \quad & l_r, \frac{I_{exit}}{I_{peak}} \\ \text{subject to} \quad & \bar{m} \leq m \\ & v \in [1500, 2000]\ m/s,\ V_c \in [3.25, 6.5]\ kV \end{aligned} \tag{8}$$

A. Constants and Constraints

As [16] suggests, choosing a linear current density in the range of 30 to 42 kA/mm is preferable to minimize the probability of transition. The optimization is done separately for the various λ values: 0.2, 0.3, and 0.4. The parameters are presented in Table IV.

B. Aim and Methodology

Each individual has three genes; m, v_{exit}, and capacitor voltage denoted as V_c. The upper and lower limits of the variables are demonstrated in Table V. The less V_c provides

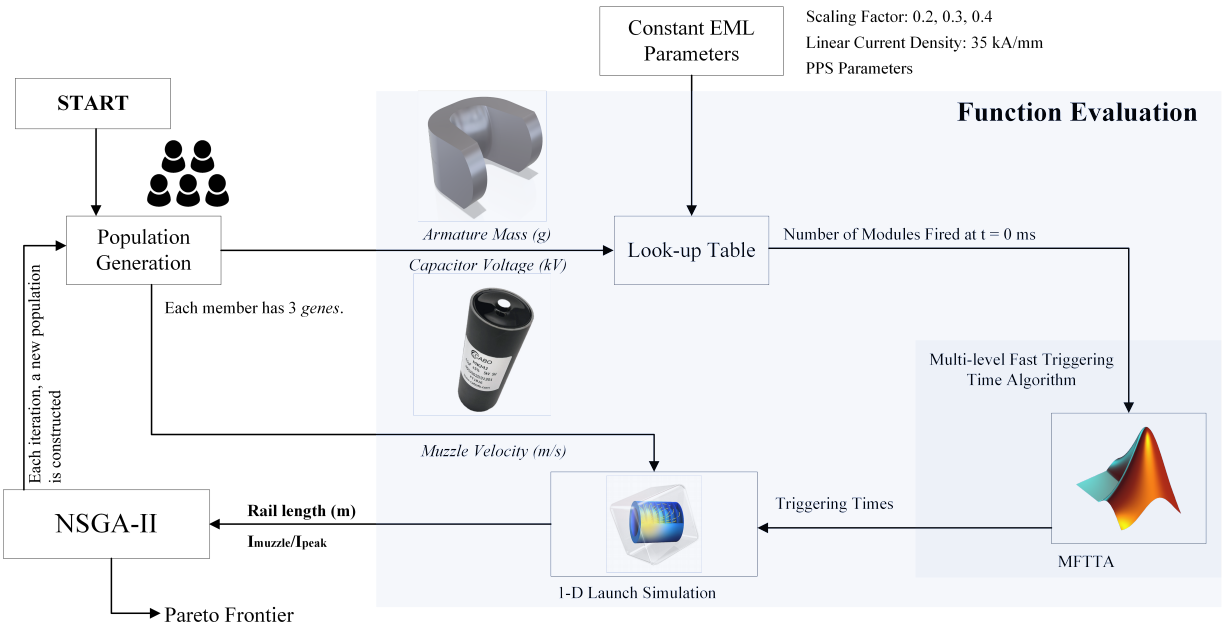

Fig. 5. The flowchart of the optimization algorithm.

TABLE IV
EML SYSTEM PARAMETERS

Linear Current Density (J)	35 kA/mm
λ[1]	0.2, 0.3, 0.4
Pre-load Distance	0.3 m

[1] When $\lambda = 0.2$, h is 10 mm, which results with tiny rails. Also, when the λ is equal to 0.5, the h is 25 mm, the same as EMFY-1 (the first prototype of ASELSAN's railgun). Thus we have investigated the scaling factors between $\lambda = 0.2$ and $\lambda = 0.4$.

TABLE V
OPTIMIZATION VARIABLES

Parameter	**Min. Value**	**Max. Value**
Armature Mass (m)	$\bar{m}$	200 g
Armature Exit Velocity (v_{exit})	1500 m/s	2000 m/s
Capacitor Voltage (V_c)	3.25 kV	6.50 kV

flexibility to obtain the various I_{peak}, with a cost of more module is needed.

The flowchart of the optimization is shown in Fig 4. The optimization is repeated for each λ. It includes V_c and the number of modules fired at time t=0 (N_{t0}) to reach the desired peak current. V_c and m are inputs for the look-up table, and it gives (N_{t0}) as the output only for the specified m.

After deciding N_{t0}, the optimization algorithm for each λ divides into three parts: N=0, N=1, and N=2 where N states the number of modules fired after t=0. MFTTA is used to find the most suitable triggering times [17]. Having larger N helps to build pulsed-shaped current with a cost of need for more PPS modules.

VI. RESULTS

Optimizations has well-behaved convergence with 50 iterations and 100 populations. Results are demonstrated in Fig 6. It is found that N=0 is more advantageous than others in all λ cases. This is because firing all modules at start results in maximum efficiency. The PPS's rise time should be shorter if all parts are scaled. However, when the existing PPS is used, the current waveform until the rise time acts like a pulse width, and hence the efficiency reduces. This means that I_{exit} is higher for $N > 0$, which results in an increase in the ratio of the exit current to the peak current.

In Fig 7, the optimization results can be seen for the cases with N=0, N=1, and N=2, respectively. As the figures show, in all cases with N, λ=0.4 is more advantageous than the other cases. Since the existing PPSs are used, the scaled model with the higher λ gives a better Pareto front and is more advantageous to use. However, as λ increases, the cost of the prototype increases.

VII. CONCLUSION

This article optimises EML scaling for efficiency and energy density. Scaling maintained T, B, and S regardless of geometry. Scaled EMLs can be produced with rail lengths from 1 to 3 metres. As existing PPS is utilised to reduce costs of manufacture, scaled models have lower efficiency than reference models. The study's observations are below:

1) As N increases, Pareto frontiers get worse. N increases the pulse width of the current. Since the current rise time does not change using with the same PPS, the armature of the scaled model experiences more current than it should. Therefore, pulsed with should be kept minimum if the existing full-scale PPS are used. As a result, it is

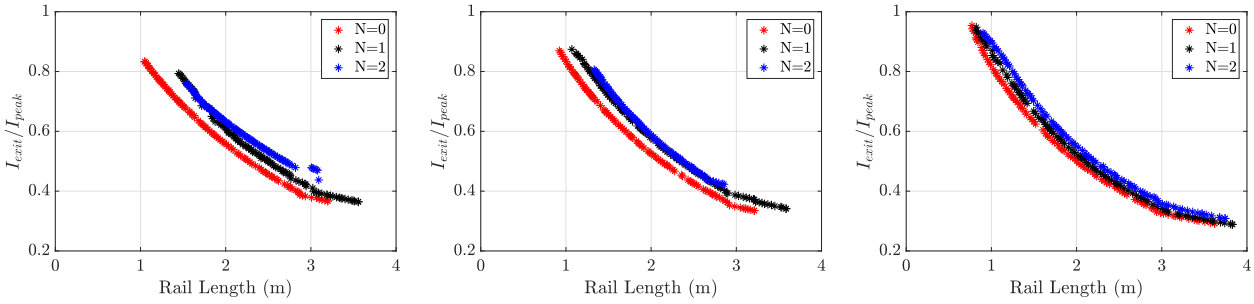

(a) λ=0.2 (b) λ=0.3 (c) λ=0.4

Fig. 6. Pareto frontiers for λ=0.2 (a), λ=0.3 (b) and λ=0.4 (c). Red, black and blue lines represent N=0, N=1 and N=2, respectively.

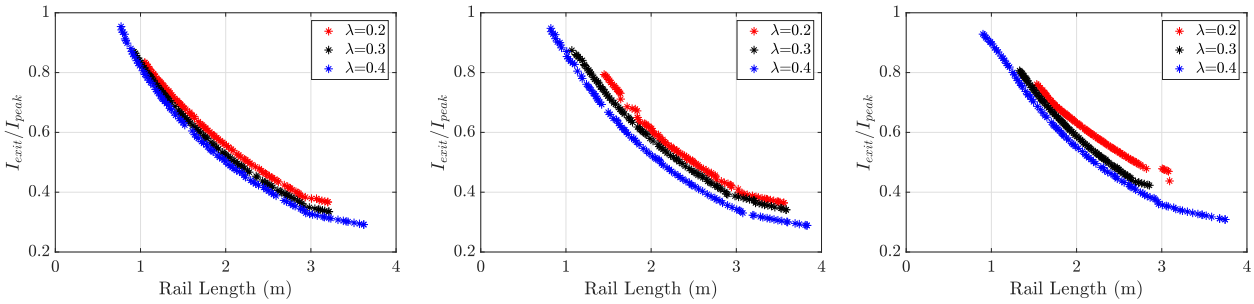

(a) N=0 (b) N=1 (c) N=2

Fig. 7. Pareto frontiers for N=0 (a), N=1 (b) and N=2 (c). Red, black and blue lines represent λ=0.2, λ=0.3 and λ=0.4, respectively.

obtained that N=0 case is more advantageous than N=1 and N=2.

2) As λ increases, Pareto frontiers get better. Since existing PPS in the reference model is used in the optimization, the required PPS characteristics are closer in scaled models as λ increases. Also, the results show that λ=0.4 is more advantageous than λ=0.2 and λ=0.3.

Scaling reduces experiment-driven EML research expenses. This obviates the necessity for new, proportionally adjusted PPS. The 250 kJ capacitive PPS, has been designed and manufactured by ASELSAN is utilised in a scaled-down iteration of the concave-caliber EMFY-4 launcher, which has been recently constructed.

REFERENCES

[1] Nail Tosun, Mustafa Karagöz, Ferhat Yurdakonar, Görkem Gülletutan, Baran Yıldırım, and Ozan Keysan. Muzzle voltage experiments of the emfy-3 launcher. *IEEE Transactions on Plasma Science*, 50(10):3434–3442, 2022.

[2] M. Otooni, A. Graf, C. Dunham, Ian Brown, and Xiang Yao. Surface modification of electromagnetic railgun components. *MRS Proceedings*, 316, 01 2011.

[3] R. Olsen, F. Chamberlain, and J. McClung. Railgun insulator materials test. *IEEE Transactions on Magnetics*, 22(6):1628–1632, 1986.

[4] S. Levinson, J.V. Parker, Kuo-Ta Hsieh, and Bok-Ki Kim. Electrical and thermal effects of rail cladding. *IEEE Transactions on Magnetics*, 35(1):417–422, 1999.

[5] H.D. Yun. Em gun scaling relationships. *IEEE Transactions on Magnetics*, 35(1):484–488, 1999.

[6] K.T. Hsieh and B.K. Kim. One kind of scaling relations on electromechanical systems. *IEEE Transactions on Magnetics*, 33(1):240–244, 1997.

[7] Yadong Zhang, Jiangjun Ruan, and Ying Wang. Scaling study in a capacitor-driven railgun. *IEEE Transactions on Plasma Science*, 39(1):215–219, 2011.

[8] Longwen Jin, Jun Li, and Bin Lei. Approximate field scaling of railgun launcher under the condition of matching projectile dynamic parameters. *IEEE Transactions on Plasma Science*, 43(9):3286–3292, 2015.

[9] Sikhanda Satapathy and Harold Vanicek. Energy partition and scaling issues in a railgun. *IEEE Transactions on Magnetics*, 43(1):178–185, 2007.

[10] Yadong Zhang, Jiangjun Ruan, Junpeng Liao, Yuanchao Hu, and Kaipei Liu. Nonlinear scaling relationships of a railgun. *IEEE Transactions on Plasma Science*, 41(5):1442–1447, 2013.

[11] V. Sung and W. G. Odendaal. Application-based general scaling in railguns. *IEEE Transactions on Plasma Science*, 41(3):590–600, 2013.

[12] Nail Tosun, Hakan Polat, Doğa Ceylan, Mustafa Karagoz, Baran Yıldırım, İbrahim Güngen, and Ozan Keysan. A hybrid simulation model for electromagnetic launchers including the transient inductance and electromotive force. *IEEE Transactions on Plasma Science*, 48(9):3220–3228, 2020.

[13] J. Kerrisk. Electrical and thermal modeling of railguns. *IEEE Transactions on Magnetics*, 20(2):399–402, 1984.

[14] Andrew Vanderburg, Francis Stefani, Alex Sitzman, Mark Crawford, Dwayne Surls, Chloe Ling, and Jason McDonald. The electrical specific action to melt of structural copper and aluminum alloys. *IEEE Transactions on Plasma Science*, 42(10):3167–3172, 2014.

[15] K. Deb, A. Pratap, S. Agarwal, and T. Meyarivan. A fast and elitist multiobjective genetic algorithm: Nsga-ii. *IEEE Transactions on Evolutionary Computation*, 6(2):182–197, 2002.

[16] F. Stefani and R. Merrill. Experiments to measure melt-wave erosion in railgun armatures. *IEEE Transactions on Magnetics*, 39(1):188–192, 2003.

[17] Nail Tosun, Hakan Polat, and Ozan Keysan. Electromagnetic launcher speed control with a multilevel fast triggering time algorithm (mftta). In *2021 IEEE Pulsed Power Conference (PPC)*, pages 1–10, 2021.